Materials Science and Engineering B 288 (2023) 116217

Contents lists available at ScienceDirect

Materials Science & Engineering B

journal homepage: www.elsevier.com/locate/mseb

Nonenzymatic electrochemical lactic acid sensor using CuO nanocomposite

M.S. Sajna [a], John-John Cabibihan [b], Rayaz A. Malik [c], Kishor Kumar Sadasivuni [a,*], Mithra Geetha [a], Johaina Khalid Alahmad [a], Dima Anwar Hijazi [a], Fatimatulzahraa Alsaedi [a]

[a] Center for Advanced Materials, Qatar University, Doha, Qatar
[b] College of Engineering, Qatar University, Qatar
[c] Weill Cornell Medicine, Qatar

ARTICLE INFO

Keywords:
Copper oxide
Lactic acid
Non-enzymatic
Sensor
Sweat

ABSTRACT

The detection of biochemical performance and health parameters using wearable sensors have gained more attention. Lactic acid (LA) sensor was developed using the simple facile method for electrochemical detection in artificial sweat. The non-enzymatic LA sensing characteristics were assessed using cyclic voltammetry and amperometry response with a three-electrode system. The CuO nanoparticles were applied to a glassy carbon electrode (GCE) as a single-step modification using the Nafion matrix. In order to examine the CuO material used to modify the glassy carbon electrode, various analytical methods were used such as Fourier transform infrared spectroscopy (FTIR), ultraviolet–visible spectroscopy (UV–Visible), and X-ray powder diffraction (XRD). The minimum detectable concentration for lactic acid was found to be 0.05 × 103 mol/l. The present investigation provides an excellent pathway for the specific detection of LA biomolecule for medical purposes by a non-enzymatic approach.

1. Introduction

Biosensors for various metabolites have been developed in recent years for surveillance applications such as clinical analysis, disease diagnosis, veterinary use, agricultural applications, industrial processing, and environmental monitoring [1–2]. In the culinary, cosmetics, pharmaceutical, leather, chemical, and other sectors, lactic acid ($CH_3CH(OH)COOH$) are frequently utilized. Tens of thousands of tons of lactic acid are consumed globally each year, and this number is predicted to rise sharply [3]. Moreover, lactic acid is an essential biomolecule found throughout the human body, with a normal blood lactate concentration ranging from 0.4 to 1.2 mmol/l. The concentration of lactic acid in human sweat, which is present in blood as well, ranges from 4 to 25 mM in a person at rest and can reach over 50 mM after vigorous exercise [4]. The creation of low-cost techniques for measuring lactic acid is crucial in this regard.

The importance of lactic acid (LA) measurement has increased recently due to its association with pathological conditions, such as shock, respiratory insufficiency, and heart disease because it is involved in glucose metabolism [5]. Lactic acidosis is a type of metabolic acidosis that occurs when the body cannot adjust to lactic acid production or utilization changes. Lactic acidosis impairs the ability of the liver and kidneys to eliminate excess acid from the body [6]. Biological fluids become acidic when lactic acid builds up faster than it can be eliminated from the body. Acid buildup adversely affects the pH balance of the body, which is meant to be slightly alkaline and never acidic. Therefore, lactic acid measurement is vital to realizing our quality of life. Aside from managing the fermentation of lactic acid bacteria strains, which are usually used to manufacture lactic acid, as well as for testing food, agricultural raw materials, etc., effective and affordable methods for measuring lactic acid can be widely used. [7].

The most precise ways to measure lactic acid involve various HPLC techniques, including ion, ion-pair, reversed-phase chromatography, and ion-exclusion [8]. Due to the difficulty of sample preparation, the requirement for costly equipment, and the need for trained workers, HPLC is not frequently utilized in ordinary practice. One disadvantage of this group of methods is the requirement to eliminate protein and carbohydrate impurities before determining lactic acid due to the incomplete exclusion of impurities from the test sample. In addition, lactic acid can be determined by an enzymatic method using the enzyme lactate dehydrogenase to convert lactic acid into pyruvate. The method is complex, expensive, and requires thoroughness [9]. Consequently, developing simple and effective techniques to measure lactic acid is essential.

* Corresponding author.
E-mail address: kishor_kumars@yahoo.com (K. Kumar Sadasivuni).

https://doi.org/10.1016/j.mseb.2022.116217
Received 21 September 2022; Received in revised form 2 December 2022; Accepted 13 December 2022
Available online 19 December 2022
0921-5107/© 2022 The Author(s). Published by Elsevier B.V. This is an open access article under the CC BY license (http://creativecommons.org/licenses/by/4.0/).

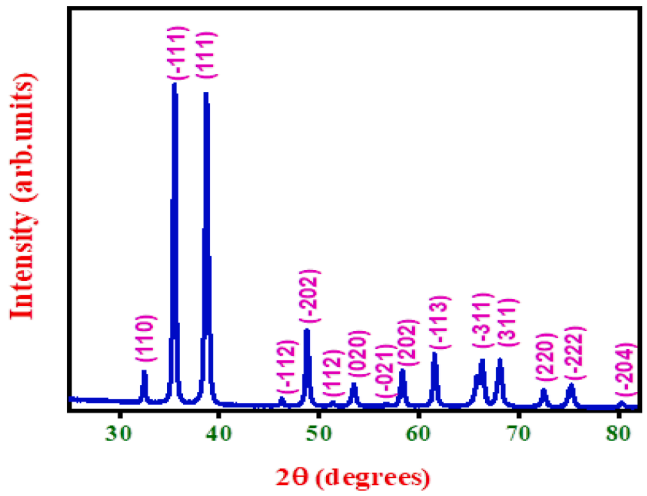

Fig. 1. XRD pattern of CuO nanoparticles.

Enzyme-based lactate biosensors have received a lot of attention. Despite their benefits, they have disadvantages, such as low reliability due to biological degradation and higher costs [10]. Hence, developing a simple, quick-response, low-cost, and dependable method of detecting Lactic acid is essential [11]. The current devices available for detecting LA are based on detecting it in blood. In contrast, detecting LA in exhaled breath, which is non-invasive and non-condensate, is not a success due to its low sensitivity [12].

The electrochemical catalytic properties of transition metal oxides and their high stability have made them very attractive for developing non-enzymatic biosensors. Nanostructured metal oxides, particularly CuO, are being investigated as sensing platforms to measure various analytes [13]. Copper oxide is a non-toxic transition metal oxide and could be a potential candidate for the future. Due to its high stability, great catalytic activity, good mechanical strength, and high thermal durability, it is a good choice for electrochemical applications. The eccrine sweat glands produce lactic acid secreted onto the skin through eccrine sweating. Today, screen-printed carbon electrodes are used in a variety of electrochemistry applications, most notably energy conversion, microelectronics, storage, chemical and biochemical sensing [14–17]. Almost all types of carbon have been placed through screen printing, with carbon black, activated carbon, and graphite is the most common. Screen printing has many benefits over other techniques. It is possible to regulate the electrode's area, thickness, and composition. Second, replicate electrodes make it possible to statistically verify the outcomes of experiments. In order to incorporate them, catalysts may also be added to the screen-printing ink.

The present work aimed to develop a simple, inexpensive, and rapid electrochemical method to determine lactic acid using a CuO-modified glassy carbon electrode. This method is advantageous in detecting lactic acid in medical applications and the quality control of foods, agricultural raw materials, etc. In this study, we developed an electrochemical biosensor that can directly detect the low-level concentration of LA in sweat.

2. Experimental

2.1. Materials and methods

Analytically ranked chemicals, including D-glucose, Nafion, Urea, Uric acid, KCl, NaCl, and L-Lactic acid, were obtained from Sigma-Aldrich Company and used without further purification. The coating materials were modified with ethanol and Nafion (coating binder). The water used during the experiments was double distilled.

Analyzing CuO was done using the following methods. To investigate the crystal structure, an X-ray diffractometer (X'PERT-Pro MPD, PANalytical Co., Almelo, Netherlands) was used under ambient conditions (Wavelength, $\lambda = 1.54$ Å). In order to validate the chemical bonding of the components, a Fourier transforms infrared (FT-IR) spectrum was acquired using crushed KBr pellets from 500 to 4000 cm^{-1} using a NicdeT 740 spectrometer. Transmission electron microscopy (TEM) was used to measure particle size. The TEM was performed on a JEM2100F (JEOL ltd., Japan) operating at 100 kV. Gatan charge-coupled device cameras (CCDs) were used to capture the digital images. Samples for TEM observation were prepared by ultrasonically dispersing powders of CuO nanoparticles in water and allowing the dispersion to drop on a copper grid. We used a twin-beam spectrophotometer, the Biochrom Libra S60, for UV–visible spectroscopy.

2.2. CuO nanoparticles preparation

Copper oxide nanoparticles were synthesized using sodium hydroxide (NaOH) as a decreasing agent and copper (II) acetate [$Cu(CH_3COO)_2{\cdot}H_2O$] as a parent during aqueous precipitation. A round-bottom flask was filled with 300 ml of copper (II) acetate solution and 1 ml of glacial acetic acid (CH_3COOH). The mixture was then heated to boiling. Into a flask, 15 ml of a 3 M NaOH solution was added. Concurrent with the color change, a black suspension formed. Three hours of boiling were spent stirring. A moist CuO precipitate was produced after the mixture was centrifuged and cooled to room temperature. The precipitate was filtered and rinsed with distilled water and pure ethanol many times. The final product was dried at 80° C for 8 h to produce CuO nanoparticles.

2.3. Electrochemical measurements

In order to test cyclic voltammetry (CV) and chronoamperometry, a Gamry potentiostat/galvanostat (Ref 600) with a three-electrode cell arrangement was used. In all voltammetry tests, the counter electrode, reference electrode, and working electrodes were all made of graphite, Ag/AgCl (3 M KCl solution), and Glassy Carbon (GC). An electrochemical cell with a capacity of 100 ml was utilized to detect LA using a three-electrode-based conventional arrangement. An artificial sweat solution with a pH of 7.4 was prepared and used as the electrolyte. LA was prepared as a 0.1 M stock solution in deionized water that was diluted into various quantities for electrochemical experiments by using the dilution procedure. Equal amounts of all interference compounds and LA were collected for the chronoamperometry testing in order to assess the CuO sensor's selectivity for LA. The working electrode was made of CuO/GCE and had a diameter of 2 mm and the electrode surface area of the sensor has been calculated as 0.0314 cm^2. The modified electrode was manually polished with aluminum powder on a polishing cloth before and after each measurement.

2.4. Electrolyte preparation and modification of GCE

Artificial sweat solution was formulated with urea (22 mM), KCl (10 mM), uric acid (25 mM), NaCl (137 mM), glucose(0.06 mM), and pH was kept at 7.4 [18–20]. Using CuO nanostructures, the glassy carbon electrode was modified as follows. Glassy carbon electrodes were cleaned with aluminum powder and deionized water several times to provide a clear surface for further modification. The GCE is left to dry in the open air for one hour following the cleaning process. An ice bath was used to sonicate 15 mg of CuO powder dissolved in 2 ml of ethanol for a half-hour. Nafion (20 μL) was added dropwise and sonicated in an ice bath for about 1 hr. On the dried active surface of the glassy carbon electrode, 10 μL of the prepared ink solution was deposited using the drop-casting method. Immediately following modification, the deposited glassy carbon electrode was left to dry in the open air for 12 h to ensure homogeneous film development. This electrode was referred to in the text as copper oxide-modified glassy carbon electrode (CuO/GCE).

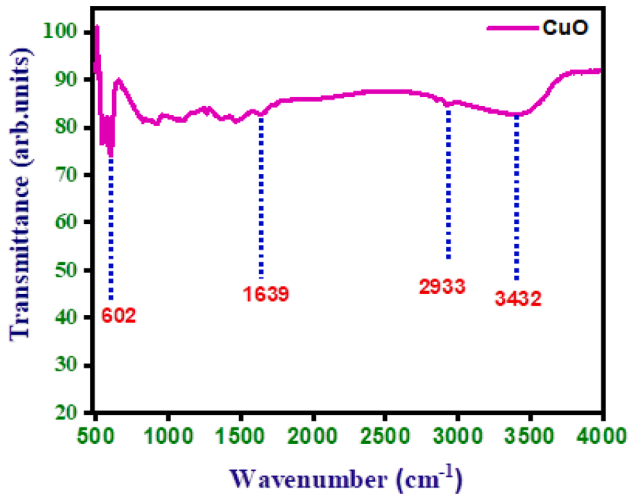

Fig. 2. FTIR spectra of the CuO nanoparticles.

3. Results and discussion

3.1. XRD analysis

The crystalline quality and purity of the cuprous oxide were studied by the powder XRD technique to identify the crystalline nature of the CuO NPs. Fig. 1 gives the XRD diffraction pattern and it shows that the reflection peaks with 2θ values were assigned as follows 32.49 (1 1 0), 35.53 (−1 1 1), 38.70 (1 1 1), 46.24 (−1 1 2), 48.73 (−2 0 2), 51.34 (1 1 2), 53.43 (0 2 0), 56.69 (−0 2 1), 58.31 (2 0 2), 61.51 (−1 1 3), 66.24 (−3 1 1), 68.06 (3 1 1), 72.39 (2 2 0), 75.22 (-2 2 2), 80.19 (−2 0 4).

The sample exhibits monoclinic lattice characteristics with values of a = 0.4685 nm, b = 0.3425 nm, and c = 0.5130 nm, which is compatible with JCPDS card number 45–0937, as well as a significant peak at the 35° position with (1 1 1), indicating that the sample is of high crystalline quality. Peak positions and (h k l) values are shown in Fig. 1. However, several of the (h k l) values start negative, indicating that they are moving in the wrong direction. The fact that all of the peaks are sharply defined suggests that the sample is free of crystallinity impurities. The reference ICDD: 98–062-8616 of copper oxide is perfectly matched to copper oxide diffraction patterns [21–23]. The average crystallite size of the CuO NPs was determined using the Scherrer equation, and XRD examination shows that the CuO nanoparticles are crystalline.

$$L = 0.9\lambda/\beta cos\theta \quad (1)$$

where is the X-ray wavelength, is the FWHM measures line broadening, and is the Bragg angle in degrees. L is the crystallite size in nm. A 27.5 nm average size was discovered. CuO nanostructures' crystallinity with the monoclinic phase was confirmed by the lack of an extra peak for commonly occurring impurities, such as Cu2O or Cu(OH)2, in the XRD pattern. Overall, high crystallinity was seen in the XRD patterns.

3.2. FTIR analysis

Because each chemical bond has a specific energy absorption band, FTIR spectroscopy is a powerful tool for detecting functional groups in molecules. It can also be used to learn about the structure and bonds of a complex to determine how strong and what kind of bonds it has.

The copper oxide's FTIR spectrum is displayed in Fig. 2. The bands at 2933 and 3432 cm-1 clearly show the symmetric and asymmetric stretching vibrations of the O–H bonds. The stretching vibration of the Cu–O bond is indicated by the peak at 1639 cm-1 [23]. Bands at 523 cm-1 and 1011 cm-1 suggest various bending vibrational modes of the Cu–O bond of copper (II) oxide nanoparticles [24–26].

3.3. Transmission electron microscopy analysis

The TEM image of CuO aggregates can be seen in Fig. 3. The resultant

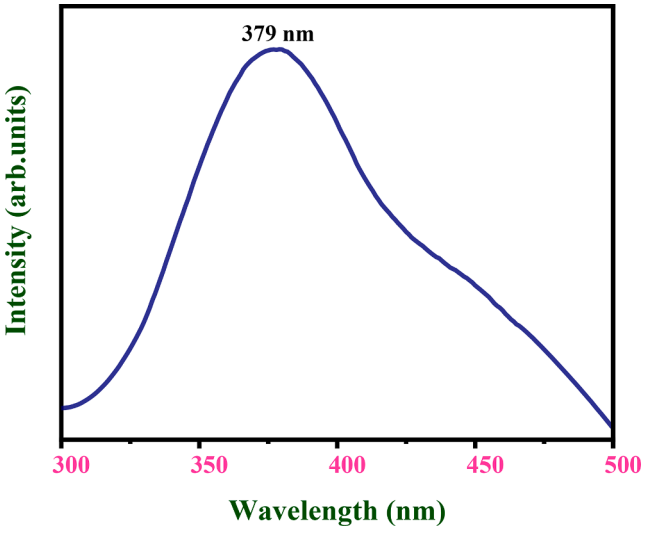

Fig. 4. UV absorption and energy band gap of CuO nanoparticles.

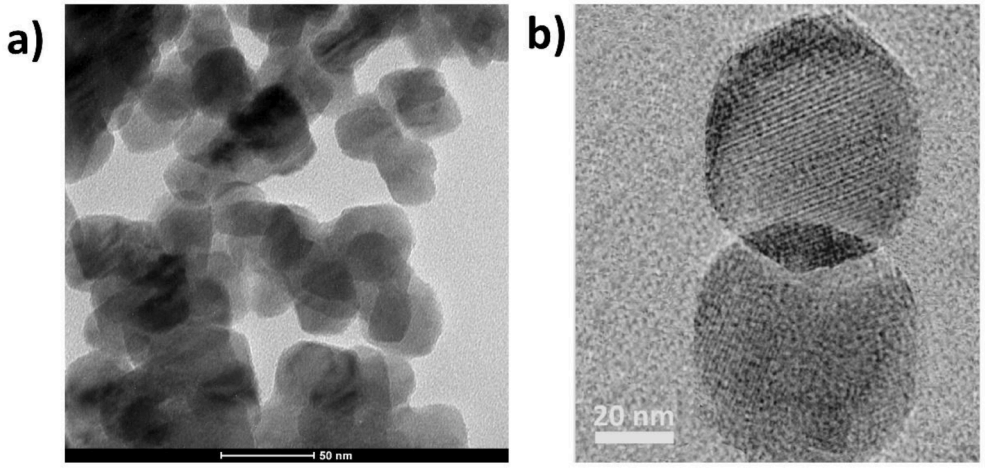

Fig. 3. A) tem micrographs of CuO b) HRTEM micrographs of CuO.

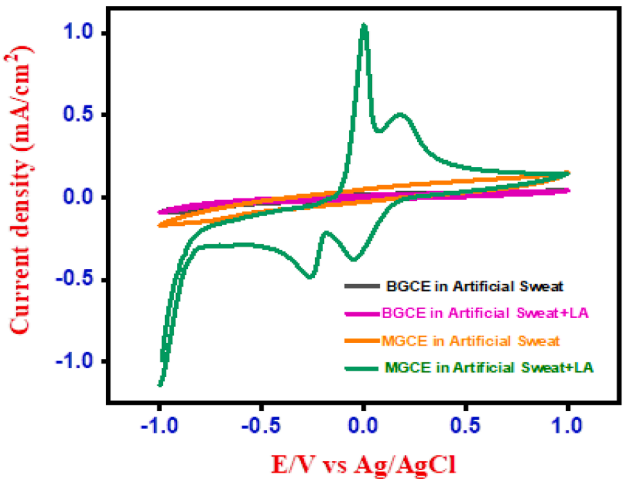

Fig. 5. Cyclic voltammetry response of CV response of bare glassy carbon electrode (BGCE) and CuO modifed GCE electrode (MGCE) with and without the presence of Lactic acid (LA) analyte in artificial sweat at a scanning rate of 100 mVs^{-1}.

nanoparticle shape and size were determined via TEM. We assessed the crystalline nature and capping of these particles. The particles had a diameter ranging between 25 and 30 nm. CuO forms CuO nanoparticles with a rather high aggregation state, as demonstrated by TEM pictures. Additionally, the TEM investigation shows that the samples' copper oxide has crystallized.

3.4. Absorption and bandgap analysis

One of the essential fundamental aspects of disclosing the energy band gap and optoelectronic applications is their optical absorption characteristics. The UV–visible absorbance spectra of CuO nanostructures were recorded by ultrasonically dispersing them in de-ionized water, shown in Fig. 4. UV–visible absorption spectrum gives a wide absorption band at 379 nm, which is characteristic of CuO particles[27]. Theoretically, the bandgap energy can be evaluated from the equation E = h υ, where h is the plank's constant (6.626 × 10–34 m^2kg/s) and υ = c/λ; c is the velocity of light and λ is the peak wavelength obtained from the absorption spectrum. The bandgap energy for CuO NPs was calculated for 3.3 eV according to the equation.

3.5. Cyclic voltammetric measurements of lactic acid

The cyclic voltammetric response of a bare glassy carbon electrode (BGCE) and a CuO-modified glassy carbon electrode (MGCE) with and without lactic acid at a scanning rate of 100 mVs^{-1} towards artificial sweat is shown in Fig. 5. In both cases, the BGCE does not show any appreciable change in the current response to artificial sweat. In the same way, no apparent peaks could be found for the CV curve for a CuO/GCE without the lactic acid. The cyclic voltammetry technique is used to establish the potential ranges of the different electrochemical reactions occurring during the electrochemical oxidation of CuO material and subsequent electroreduction in the artificial sweat solution. There observed two well-defined anodic peaks at 0.2 and −0.04 V which is related to the formation of Cu_2O and $CuO/Cu(OH)_2$. The reverse potential scan shows three cathodic peaks. The potential values at which these electroreduction peaks are observed depending on the extent of the previous anodic sweep. Reduction peaks at −0.06 V and −0.7 V can be assigned to the electroreduction of $CuO\text{-}Cu(OH)_2$ to Cu_2O, and Cu_2O to Cu, respectively [28]. The cathodic peak at −0.3 V is observed only in carbonate-containing aqueous solutions and is associated with the electroreduction of a Cu carbonate-Cu hydroxide layer formed at potentials more positive than 0 V [29]. In the presence of LA, obtained a current response and a high-intensity peak current density of −0.04 V for the MGCE. In the present evaluation of LA sensing, this −0.04 V potential is used further for amperometry/calibration curves. The increased loop area obtained indicates that the MGCE is suitable for detecting lactic acid in artificial sweat. This plot demonstrates the excellent electrocatalytic properties of CuO on oxidizing lactic acid when compared with BGCE. The electron transfer kinetics between the analyte and the CuO material determines the peak current response in the electrochemical process. It allows the analyte analysis, namely lactic acid in sweat solution, more easily.

and efficiently.

3.6. Effect of scan rate

The electrochemical kinetics of the lactic acid in the artificial sweat solution were investigated by measuring the CV response of lactic acid using a CuO-modified glassy carbon electrode (MGCE) at varying scan speeds. The CV response of the MGCE in artificial sweat is depicted in Fig. 6(a). Lactic acid and MGCE are combined in Fig. 6(b). The graph demonstrates that when the scan rates change, the peak reduction gets larger. When the scan rate was set to 100 mV/s, the largest decrease

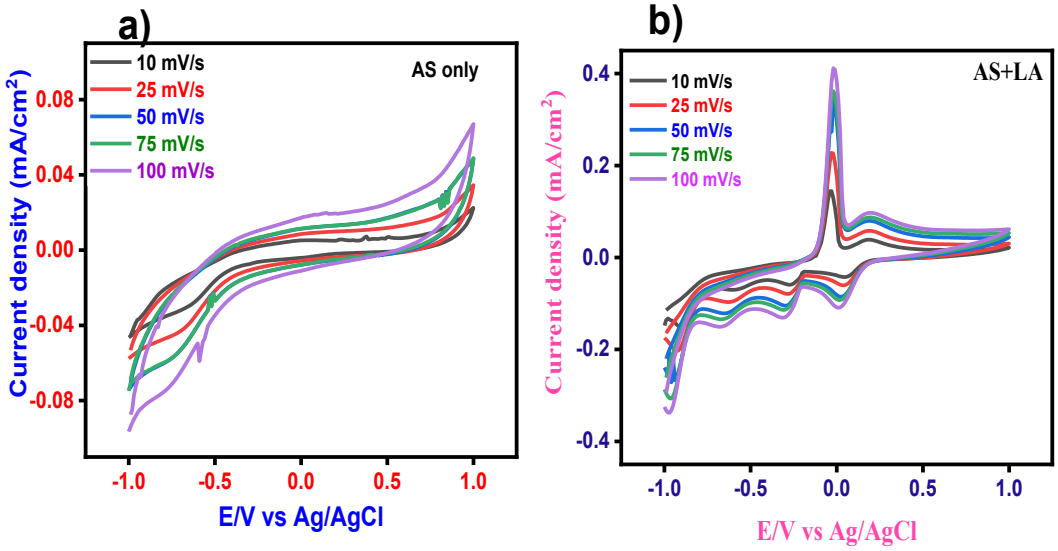

Fig. 6. CV analysis of MGCE electrode at different scan rates(a) artificial sweat only and (b) with lactic acid.

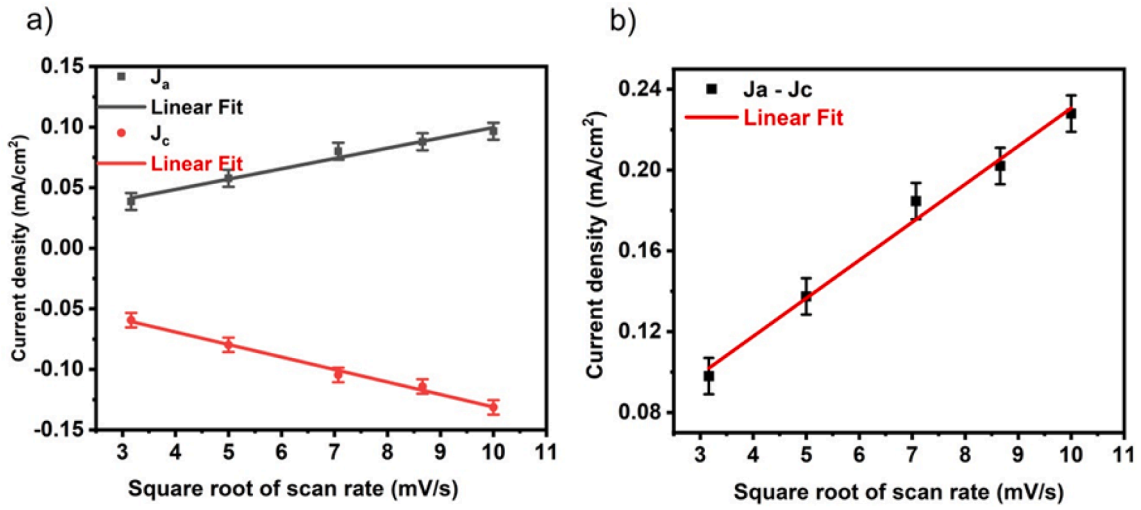

Fig. 7. (a) The Square root of scan rate vs anodic and cathodic current (b) Linear fitting of the current density differences against scan rates; from the CV analysis of CuO tailored glassy carbon electrode with the lactic acid analyte in artificial sweat medium.

peak current was recorded. The anodic and cathodic peak potentials fluctuate as the scan rate moves towards the positive and negative quadrants, which suggests a charge transfer kinetic limit.

According to Fig. 6(b), regardless of scan rate, oxidation and reduction peaks stay within their respective ranges. According to the traits of surface-bound redox sites, the cathodic and anodic peak current ratio was consistent. The increasing current density at higher scan rates confirms that the MGCE has effective catalytic activity for lactic acid detection. For the CuO customized glassy carbon electrode, the well-defined CV curves with a diffusion-controlled redox process were obtained.

The peak current and scan rate linear relation with the addition of lactic acid analyte indicates that the oxidation reaction is confined to the electrode's surface. It is clear from the well-defined redox peak current response that was obtained that electron transport during the redox reaction on the modified electrode is a diffusion control reaction (Fig. 7a). Additionally, the anodic and cathodic peak currents shift toward positive and negative potential as scan speeds rise, illuminating a quasi-reversible electron transfer reaction on the electrode surface [24].

The increase in current density was investigated by plotting redox peak current density concerning the square root of scan rate and the linear fitting of the current density differences against scan rates as given in Fig. 7(b). Regardless of the oxidation or reduction cycle, the current density plot shows a linear relationship with the square root of the scan rate. This indicates that the pace at which the electrolyte diffused to the active sites influenced the electrochemical processes. By examining the scan rate dependency of cyclic voltammetry analysis and the CuO catalyst's double-layer capacitance (Cdl) measurement, the electrochemical active surface area (EASA) of the CuO catalyst was estimated by the equation EASA = Cdl/Cs. The Cdl was calculated by plotting the anodic and cathodic current density difference (ΔJ = Ja-Jc) against the scan rate, as shown in Fig. 7(b). The fitted linear regression slope equals twice the Cdl, and for the CuO catalyst, it was determined to be 12.1 $mFcm^{-2}$, which specifies the density of the electrochemically active surface area. On a unit surface area, Cs denote the specific capacitance of conventional electrode material. According to the literature, a typical Cs value of 0.02 $mFcm^{-2}$ was employed in the computation, yielding EASA = 605 [24]. As per CV analysis, the CuO has several active sites, outstanding electrical properties, fast analyte transit kinetics, and is highly sensitive for lactic acid detection. The calibration plot of the square root of scan rate and the peak current shows the surface limited electrochemical redox process of the modified electrode.

The CuO/GCE-based lactic acid sensor's equivalent amperometric response at an applied voltage of −0.04 V is shown in Fig. 8(a). The response of the modified electrode was improved as the LA concentration was increased from 0.05 mM to 40 mM due to the increased conductivity of the catalyst. Within this linear range, lactic acid has a response time of 5 s which explains the strong electrocatalytic activity of the prepared catalyst. Due to medical conditions, lactate concentrations of up to 40 mM cover the lactate concentration range in human body fluids [2526].

Fig. 8(b) exhibits the calibration plot between lactic acid and the current density response of the CuO modified electrode. The limit of detection (LOD) was evaluated from the 3σ/m, in which σ is the standard deviation of the intercept and m represents the slope of the calibration plot. The estimated LOD of lactic acid in the artificial sweat solution was 0.04 mM from this calibration plot.

The peak current density variation concerning the lactic acid concentration is shown in Fig. 8(c), and the inset gives the CV graphs concerning it. It is evident from the graph that the CuO-modified glassy carbon electrode exhibited a linear response in the concentration range of 0.05–2.5 mM. The LOD was found to be 0.027 mM and the sensitivity of ~ 14.47 $mAmM^{-1}cm^{-2}$ is evaluated in the range of evaluation and a response time of < 5 s implied that the CuO nanoparticle had enhanced conductivity, which improves the electrocatalytic activity towards lactic acid detection. The reversible electron transfer process is verified by the linear increase in the peak current density with the increase in the lactic acid concentration.

3.7. *Reproducibility, stability, and interference effects*

The term "reproducibility" describes the consistency of results obtained using a variety of the same modified electrodes and the same measurement method. The CV responses of five different electrodes were recorded under ideal circumstances after injecting 7 mM of LA each time. The relative standard deviation (RSD) of the response currents for varied CuO MGCE was just 1.12 %, as shown in Fig. 9, indicating excellent precision and consistency of the sensor.

The current response of the 7 mM Lactic acid was recorded for 20 repetitive cv runs with a 100 mVs-1 scan rate in order to assess the stability of the as-prepared sensor with CuO modified glassy carbon electrode for the detection of lactic acid and reproducibility measurements.

The results are shown in Fig. 10. It is clear that the current response has not changed significantly after 20 cycles of continuous scanning, proving that the res as-prepared CuO/GCE sensor is reliable and stable

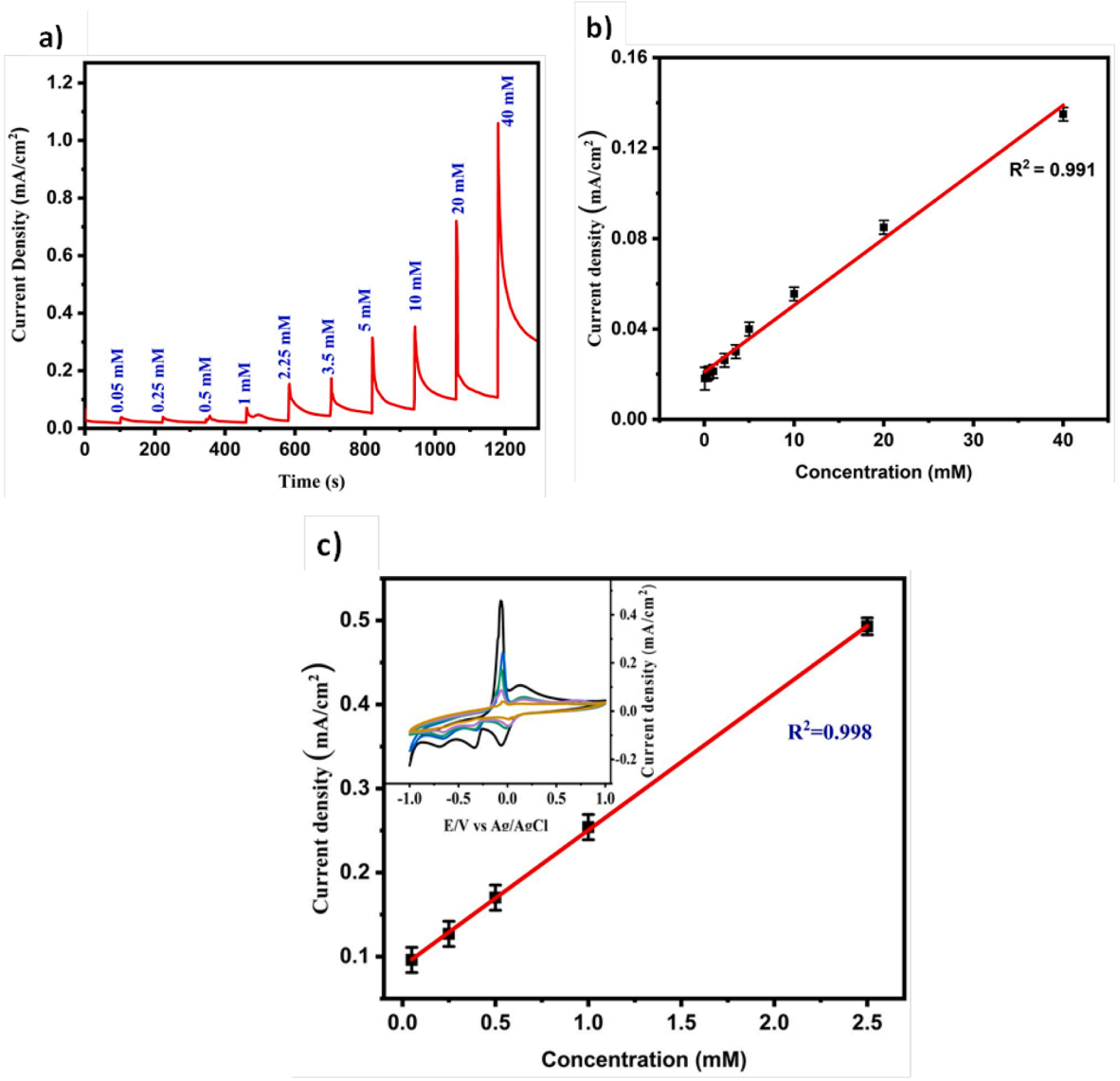

Fig. 8. (a) Chronoamperometric responses of activated non-enzymatic lactic acid sensor with progressive increase of lactic acid concentrations at −0.04 V (b) Calibration plot between the steady-state current density and the lactic acid concentration (c) The calibration curve and of CV response of CuO nanoparticles towards various lactic acid concentrations in the linear range of 0.05–2.5 mM at a scan rate of 50 mVs^{-1}. Inset: CV analysis of Modified CuO/GCE towards Lactic acid concentration variation.

for measuring lactic acid.

One of the other key parameters signifying the performance of the sensor is its repeatability. Repeatability is defined as the compatibility among consecutive readings with the same electrode. A modified GCE was used five times in a day to verify the repeatability. The relative standard deviation of the repeatability is 2.42 %, as shown in Fig. 11 suggesting that the proposed sensor has good repeatability.

Selectivity is one of the key factors in evaluating sensing devices. The amperometric measurement of various oxidizable chemicals concerning lactic acid concentration was carried out to determine the selectivity of the CuO NPs, as shown in Fig. 12. The CuO modified electrode's response of many interfering biomolecules, which are electro-active substances and are readily oxidizable like glucose, sucrose, fructose, uric acid that coexist with lactic acid in human sweat, was investigated.

The amperometric response of the electrode when 3 mM of acetone, uric acid, glucose, fructose, sucrose and lactic acid are continuously added to artificial sweat is shown in Fig. 12. It was discovered that the current response of those mentioned above electroactive interfering species is showing no significant interference, indicating that the CuO MGCE has a high selectivity for the lactic acid determination.

3.8. *Detection of L-Lactic acid using screen-printed glassy carbon electrode*

A glassy carbon working electrode (W) covered with CuO, a graphite counter electrode (A), and an Ag/AgCl reference electrode were used to create screen-printed glassy carbon electrode (SPGCE) strips (R). The electrode is supported by one or more 50 mm long, 20 mm broad, and 0.5 mm thick alumina ceramic bases. The working (W), reference (R), and auxiliary (A) electrodes were attached to this surface. The schematic depiction of a manufactured sensor is shown in Fig. 13. The three-electrode design of the flexible lactic acid sensor was created utilizing an alumina ceramic foundation. O_2 plasma etching and IPA were used to clean the alumina ceramic substrate. A layer of 3 mm diameter graphite is then screen printed to serve as the counter electrode, and a layer of 3 mm diameter Ag/AgCl is then printed to function as the reference electrode. The matching catalyst and carbon ink (0.95 g, Gwent C50905D1, Pontypool, UK) were well mixed manually for 5 min and

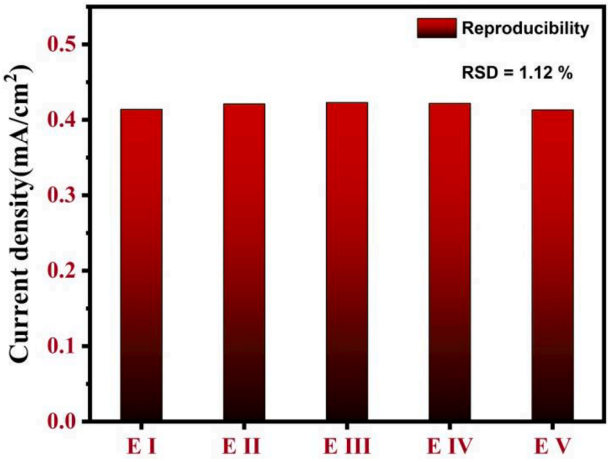

Fig. 9. Reproducibility of the CuO MGCE sensor after the addition of 7 mM of LA in artificial sweat.

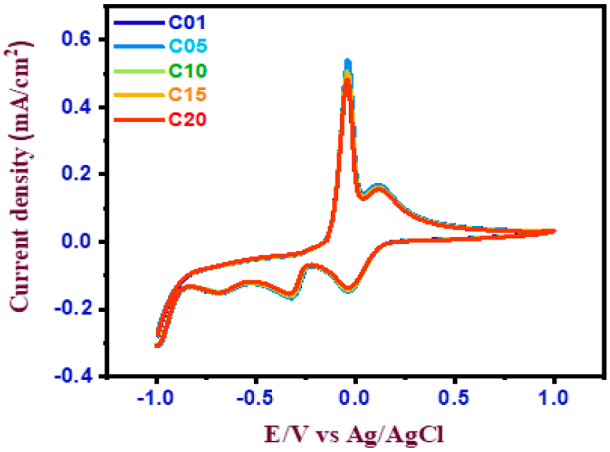

Fig. 10. Cyclic voltammetric response of MGCE in 7 mM Lactic Acid at 20 consecutive cycles at a scan rate of 100 mVs^{-1}.

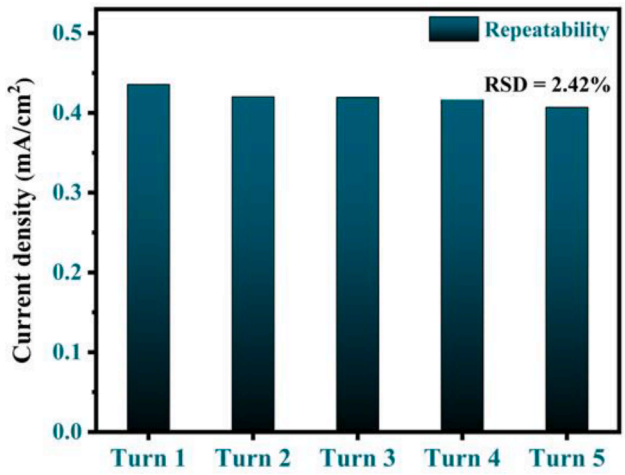

Fig. 11. Repeatability of the CV analysis of CuO/GCE sensor with 7 mM Lactic acid in artificial sweat.

then sonicated for 5 min. The resulting liquid was employed right away to create electrodes. Modified ink was screen-printed onto an inert, laser-pre-etched ceramic substrate to create functional electrodes. With

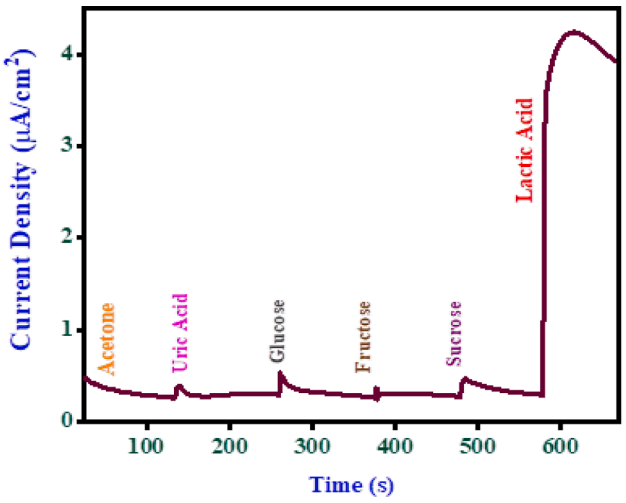

Fig. 12. Interference studies using the amperometry method for successive addition of acetone, uric acid, glucose, fructose, sucrose, and lactic acid (3 mM) at an applied potential of −0.04 V.

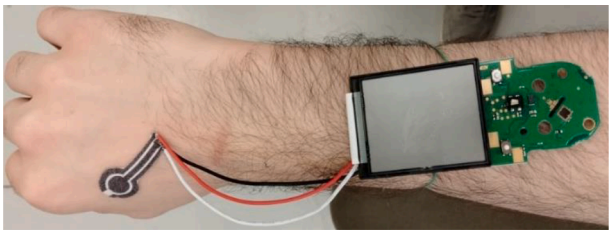

Fig. 13. Schematic representation of fabricated lactic acid detection.

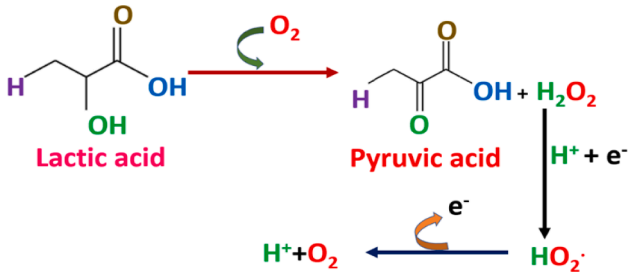

Fig. 14. Electrochemical Mechanism for the detection of Lactic acid using CuO modified GCE.

the help of the spatula included with the screen-printing apparatus (SP-200, MPM, Franklin, MA, USA and/or UL 1505 A, Tesla, Czech Republic), thick layers of the modified carbon ink were created by brushing the ink through an etched stencil onto the ceramic substrates. At 120 °C, the electrodes are dry. Between the counter electrode and the reference, the electrode will be the working electrode.

Cyclic voltammetry (CV) was used in the initial research to investigate the redox behavior at the SPCE. A tiny Auto lab potentiostat connected to a computer was used to conduct voltammetric measurements. The tests were carried out in a wall-jet cell that was specially made and contained an electrode strip. Regarding lactic acid concentration, supporting electrolyte pH, potential, and scan rate, the respective current response has been assessed. These investigations demonstrated that the electrode had a linear response with acceptable reproducibility in the concentration range of 0.05–2.5 mM. The detection threshold was discovered to be 0.027 mM. To determine the great selectivity of the electrode, an interference investigation was also conducted in the

Table 1
L-Lactic acid detection by various sensors: A comparison.

Material/ Composite	Sensor Type	pH	Electrolyte	Sensitivity ($mAmM^{-1}cm^{-2}$)	LOD (mM)	Detection Range (mM)	Response/ Delay (s)	Ref.
AuPtNPs functionalized MoS_2 nanosheet	Non–enzymatic	7.4	0.01 M (PBS) + 5 mM[$Fe(CN)_6]^{3-/4-}$ & 0.1 M KCl.	–	0.00033	0.005–3	< 15	[30]
Multi-walled CNT/Pt nanoparticle modified GCE	Enzymatic	6.4	PBS	0.06235	0.0003	0.2–2.0	< 5	[31]
Hydrogen titanate (H2Ti3O7) nanotubes	Enzymatic	7.4	10 mM PBS	0.00024	0.2	0.5–14	5	[32]
NiO NPs/GCE	Non-enzymatic	–	0.1 M NaOH in deionized water	–	0.0057	0.005–5	–	[33]
CuO MWCNT	Non-enzymatic	5.7–8	Phosphate buffer	0.000633	$88.5x10^{-8}$	$10x10^{-5}$-10.0	5	[34]
ZnO nanotetrapods	Enzymatic	7.4	PBS	0.028	0.0012	0.0036–0.6	10	[35]
MWCNT)-polypyrrole core–shell NW	Non-Enzymatic	–	0.1 M Na_2SO_4	0.0029	0.051	1–15	–	[36]
CuO	Non-Enzymatic	7.4	Artificial Sweat	14.47	0.04	0.05–40	< 5	Work

presence of high concentrations of acetone, uric acid, glucose, fructose, and sucrose.

Lactic acid in human sweat was effectively determined using this technique. The apparatus utilizes capillary action to draw perspiration into a microfluidic chamber that is filled with an alkaline solution through a tiny input. The technique prevents the wearer's body from coming into direct touch with the solution, which is crucial to take into account because alkaline solutions can harm the skin. Sweat contains lactic acid molecules, and when those molecules interact with the solution, a chemical is funneled into the electrode. When that substance interacts with the CuO, an electrical signal is created.

It is possible to determine the amount of lactic acid in the sweat by measuring the strength of that signal with an external or built-in device. In order to test the device, a skin-safe glue was used to attach the sensor to a volunteer's arm. Readings were taken shortly after the subject engaged in a brief exercise session that resulted in a minor amount of sweat. The procedure for electrochemically exposing L-Lactic acid by CuO is shown in the accompanying diagram. L-lactic acid was electro-oxidized into pyruvic acid and hydrogen peroxide in the presence of oxygen.

In synthesis, H_2O_2 was converted into an unstable intermediate, releasing one electron and proton. The intermediate molecule was converted into one oxygen and proton with the release of an electron (see Fig. 14). In the CuO customized GCE sensor, these released electrons resulted in electrochemical responses for detecting L-Lactic acid. Table 1 displays the electrochemical sensor parameters for L-Lactic acid detection by various electrochemical sensors as given below.

4. Conclusions

In conclusion, this study details the efficiency of CuO for the modification of GCE to create a novel nonenzymatic amperometric sensor for the detection of lactic acid. CuO nanoparticles were successfully synthesized by the aqueous precipitation method. Cyclic voltammetry (CV) experiment for the CuO-modified GCE in artificial sweat solution was carried out to investigate the efficiency of the MGCE electrode. The proposed enzyme-free sensor exhibits linear responses to lactic acid concentration, is convenient, has high selectivity, and requires no special storage conditions. Electrochemical assays showed that modified CuO/GCE has a strong electrocatalytic activity for the oxidation and reduction of lactic acid. Compared to many other reported sweat lactic acid sensors, the present investigation mainly covers and goes beyond the normal lactic acid concentration range in sweat without physical activity (0.05–40 mM); and hence can be used as a significant approach for detecting lactic acidosis due to medical condition non-invasively. The XRD results showed that the material exhibited mainly reflection patterns of CuO, and no other impurity was present. In addition, there is no impact from common interfering substances such as urea, uric acid, acetone, fructose, sucrose, and glucose.

Data availability

All the data retrieved from this study were included in this manuscript.Other extra data if need will be made available on request.

Declaration of Competing Interest

The authors declare that they have no known competing financial interests or personal relationships that could have appeared to influence the work reported in this paper.

Data availability

Data will be made available on request.

Acknowledgment

This work was supported by the Qatar National Research Fund under NPRP11S-0110-180247. The statements made herein are solely the responsibility of the authors.

References

[1] S. Imani, et al., A wearable chemical–electrophysiological hybrid biosensing system for real-time health and fitness monitoring, Nat. Commun. 7 (1) (May. 2016.) 1–7.
[2] F. Alam, et al., Lactate biosensing: The emerging point-of-care and personal health monitoring, Biosens. Bioelectron. 117 (Oct. 2018) 818–829.
[3] D.H. Kim, et al., "Flexible and Stretchable Electronics for Biointegrated Devices" 14 (Jul. 2012) 113–128.
[4] M.M. Pribil, G.U. Laptev, E.E. Karyakina, A.A. Karyakin, Noninvasive Hypoxia Monitor Based on Gene-Free Engineering of Lactate Oxidase for Analysis of Undiluted Sweat, Anal. Chem. 86 (11) (2014) 5215–5219.
[5] L.N. Borshchevskaya, et al., Spectrophotometric determination of lactic acid, J. Anal. Chem. 71 (8) (2016) 755–758.
[6] H.A. Favre, et al., Nomenclature of Organic Chemistry, Nomencl. Org. Chem. (Dec. 2013).
[7] P. Lavermicocca, et al., Editorial: Lactic Acid Bacteria Within the Food Industry: What Is New on Their Technological and Functional Role, Front. Microbiol. 12 (Jul. 2021) 1946.
[8] S. M. Ameen et al., "Lactic Acid in the Food Industry," 2017.
[9] R. Michalski, et al., "Ion chromatography and related techniques in carboxylic acids analysis, Crit. Rev. Anal. Chem. 51 (6) (2021) 549–564.
[10] O.M. Istrate, et al., Amperometric L-Lactate biosensor based upon a gold nanoparticles/reduced graphene oxide/polyallylamine hydrochloride modified screen-printed graphite electrode, Chemosensors 9 (4) (2021) 74.
[11] Z.H. Ibupoto, et al., Electrochemical L-Lactic Acid Sensor Based on Immobilized ZnO Nanorods with Lactate Oxidase, Sensors 12 (3) (Feb. 2012) 2456–2466.
[12] R. Monošík, et al., A rapid method for determination of l-lactic acid in real samples by amperometric biosensor utilizing nanocomposite, Food Control 23 (1) (Jan. 2012) 238–244.

[13] J. Wang, et al., Amperometric biosensors for clinical and therapeutic drug monitoring: a review, J. Pharm. Biomed. Anal. 19 (1–2) (Feb. 1999) 47–53.
[14] G.J. Kost, et al., "New Whole Blood Analyzers and Their Impact on Cardiac and Critical Care" 30 (2) (2008) 153–202.
[15] Parra, et al., Design and characterization of a lactate biosensor based on immobilized lactate oxidase onto gold surfaces, Anal. Chim. Acta. 555 (2) (Jan. 2006) 308–315.
[16] L.W. Andersen, et al., Etiology and Therapeutic Approach to Elevated Lactate Levels, Mayo Clin. Proc. 88 (10) (Oct. 2013) 1127–1140.
[17] S. Nations, et al., Subchronic and chronic developmental effects of copper oxide (CuO) nanoparticles on Xenopus laevis, Chemosphere., vol. 135, pp. 166–174, Sep. 2015.
[18] B. Devi, et al., Novel synthesis and characterization of CuO nanomaterials: Biological applications, Chinese Chem. Lett. 25 (12) (Dec. 2014) 1615–1619.
[19] D.M. Tobaldi, et al., Photo-electrochemical properties of CuO–TiO2 heterojunctions for glucose sensing, J. Mater. Chem. C 8 (28) (Jul. 2020) 9529–9539.
[20] J.A. Buledi, et al., CuO Nanostructures Based Electrochemical Sensor for Simultaneous Determination of Hydroquinone and Ascorbic Acid, Electroanalysis 32 (7) (Jul. 2020) 1600–1607.
[21] S. Paramparambath, et al., Nonenzymatic Electrochemical Sensor Based on CuO-MgO Composite for Dopamine Detection, IEEE Sens. J. 21 (22) (Nov. 2021) 25597–25605.
[22] P. Balasubramanian, et al., Ultrasensitive non-enzymatic electrochemical sensing of glucose in noninvasive samples using interconnected nanosheets-like NiMnO3 as a promising electrocatalyst, Sensors Actuators B Chem. 299 (Nov. 2019), 126974.
[23] V. Sudha, et al., Structural and morphological tuning of Cu-based metal oxide nanoparticles by a facile chemical method and highly electrochemical sensing of sulphite, 111, Feb. 2021, Sci. Rep. 11 (1) (2021) 1–12.
[24] R. Ahmad, et al., Highly Efficient Non-Enzymatic Glucose Sensor Based on CuO Modified Vertically-Grown ZnO Nanorods on Electrode, 71, Jul. 2017, Sci. Rep. 7 (1) (2017) 1–10.
[25] K. Krishnamoorthy, et al., Simultaneous determination of dopamine and uric acid using copper oxide nano-rice modified electrode, J. Alloys Compd. 748 (Jun. 2018) 338–347.
[26] P.K. Raul, et al., CuO nanorods: a potential and efficient adsorbent in water purification, RSC Adv. 4 (76) (Sep. 2014) 40580–40587.
[27] K. Velsankar et al., Ecofriendly green synthesis, characterization and biomedical applications of CuO nanoparticles synthesized using leaf extract of Capsicum frutescens, J. Env. Chem.Eng. 9(5), pp.106299.
[28] M.R. Gennero De Chialvo, J.O. Zerbino, S.L. Marchiano, et al., Correlation of electrochemical and ellipsometric data in relation to the kinetics and mechanism of Cu_2O electroformation in alkaline solutions, J. Appl. Electrochem. 16 (1986) 517–526.
[29] M. Pérez Sánchez, R.M. Souto, M. Barrera, S. González, R.C. Salvarezza, A.J. Arvia, "A mechanistic approach to the electroformation of anodic layers on copper and their electroreduction in aqueous solutions containing $NaHCO_3$ and Na_2CO_3, Electrochim. Acta 38 (5) (1993) 703–715.
[30] B.K. Shrestha, et al., In situ synthesis of cylindrical spongy polypyrrole doped protonated graphitic carbon nitride for cholesterol sensing application, Biosens. Bioelectron. 94 (Aug. 2017) 686–693.
[31] S. Kim, et al., Highly sensitive non-enzymatic lactate biosensor driven by porous nanostructured nickel oxide, Ceram. Int. 45 (17) (Dec. 2019) 23370–23376.
[32] X. Cui, et al., Highly sensitive lactate biosensor by engineering chitosan/PVI-Os/CNT/LOD network nanocomposite, Biosens. Bioelectron. 22 (12) (Jun. 2007) 3288–3292.
[33] H. Xiao, et al., Non-enzymatic lactic acid sensor based on AuPtNPs functionalized MoS2 nanosheet as electrode modified materials, J. Electroanal. Chem. 903 (Dec. 2021), 115806.
[34] J. Huang, et al., Development of an amperometric l-lactate biosensor based on l-lactate oxidase immobilized through silica sol–gel film on multi-walled carbon nanotubes/platinum nanoparticle modified glassy carbon electrode, Mater. Sci. Eng. C. 28 (7) (Aug. 2008) 1070–1075.
[35] M. Yang, et al., A lactate electrochemical biosensor with a titanate nanotube as direct electron transferpromoter, Nanotechnology 19 (7) (Jan. 2008), 075502.
[36] Y.M. Choi, H. Lim, H.-N. Lee, Y.M. Park, J.-S. Park, H.-J. Kim, Selective Nonenzymatic Amperometric Detection of Lactic Acid in Human Sweat Utilizing a Multi-Walled Carbon Nanotube (MWCNT)-Polypyrrole Core-Shell Nanowire, Biosensors 10 (2020) 111.